JOURNAL OF MATERIALS SCIENCE 31 (1996) 5953–5960

Effect of shot peening on the fatigue and fracture behaviour of two titanium alloys

B. R. SRIDHAR, K. RAMACHANDRA
Gas Turbine Research Establishment, Bangalore 560 093, India
K. A. PADMANABHAN
Department of Metallurgical Engineering, Indian Institute of Technology, Madras 600 036, India

The fatigue and fracture behaviour of two titanium alloys, the near-alpha IMI-685 and alpha-beta IMI-318, were studied in the machined and polished (MP) as well as the machined, polished and shot (glass-bead) peened (MPS) conditions. Glass-bead peening reduced the room-temperature as well as the high-temperature (450 °C) fatigue life of alloy IMI-685 at high stress amplitudes, σ_a, approaching the proof stress, σ_{ps}, of the material (LCF region). When the applied stress amplitude (0–770 MPa, HCF region) was comparable to the peen-induced peak longitudinal residual stress, σ_{LP}, i.e. $(\sigma_{LP}/\sigma_a) = 0.92$, an improvement in the room-temperature fatigue life of IMI-685 was observed. When the (σ_{LP}/σ_a) ratio was less than this value, decreases in the fatigue life were seen. The room-temperature fatigue behaviour of IMI-318 at high stress amplitudes was similar to that of IMI-685. The decrease in the fatigue life of this alloy, at a stress amplitude (770 MPa) where improvement was observed for IMI-685, could be attributed to the higher relaxation of peen-induced residual stresses in IMI-318 compared with IMI-685. Glass-bead peening improved the high-temperature (450 °C) fatigue life of IMI-685 at a low stress amplitude (465 MPa; $(\sigma_a/\sigma_{PS}) = 0.87$). The crack-initiation sites in the MP and the MPS conditions were at the surface for both the alloys. However, fracture in the surface layers of the alloys appeared more brittle in the peened (MPS) rather than in the unpeened (MP) condition.

1. Introduction

Titanium alloys, near-alpha IMI-685 (Ti–6Al–5Zr–0.5Mo–0.25Si, wt %) and the alpha-beta IMI-318 (Ti–6Al–4V) find applications in gas turbine engines. The microstructure of IMI-685 consists of acicular α (hcp) in basket-weave form, separated by thin layers of β (bcc). IMI-318, on the other hand, comprises equiaxed α grains with the β phase located at α grain boundaries [1].

The present work was concerned with the effect of shot peening with glass beads on the fatigue and fracture behaviour of these two alloys.

2. Experimental procedure

The alloys were supplied by M/S Firth Derihon Limited, UK, in the form of test segments of forgings of compressor discs. Flat and round fatigue test specimens (Fig. 1a, b) were fabricated according to ASTM specification E 466-76 [2]. The surfaces were polished down to 500 grade using SiC emery paper. They were then shot peened at a pressure of 480 kPa using glass beads (0.1–0.2 mm diameter) suspended in water (peening intensity 35 N).

The specimens were mechanically gripped on an MTS servo-hydraulic machine and subjected until fracture to constant stress amplitude axial fatigue.

The stress ratio, $R = (\sigma_{min}/\sigma_{max})$, was maintained at zero, where σ_{min} and σ_{max} are, respectively, the minimum and maximum stress applied in the fatigue tests. Several stress ranges were used but the frequency was always 2.0 Hz. The test temperatures were room temperature (25 °C), 200 and 450 °C. The number of cycles of failure was recorded in each case. The fracture surfaces were subjected to qualitative scanning electron microscopy.

3. Results

3.1. Residually stressed layers

Fig. 2, corresponding to the minimum cross-section in the shot-peened hour-glass-shaped flat and round specimens of IMI-685, shows areas under compressive residual stresses. In the case of the longitudinal residual stress, σ_L, the depth of this compressed layer was about 0.7 mm [1]. If the remaining area is assumed to be under tension, the ratio A_t/A_c works out to 1.6 and 1.4 for the flat and round specimens, where A_t is the area under tension and A_c is the area under compression.

0022–2461

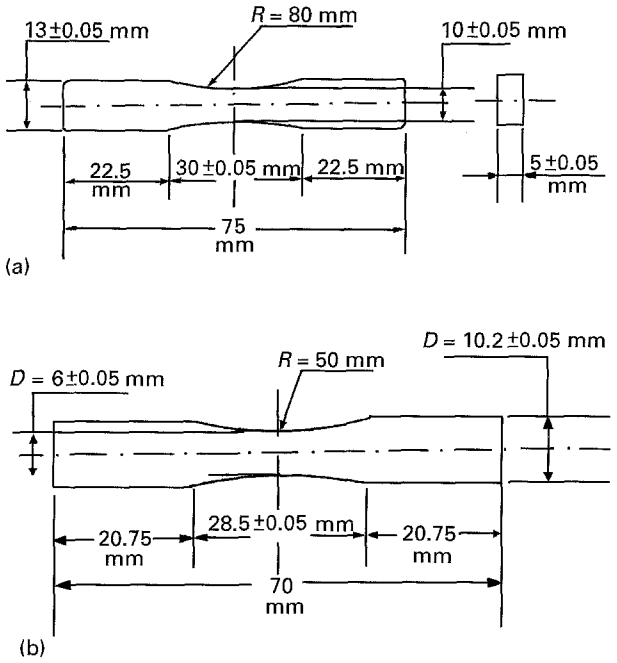

Figure 1 (a) Flat, and (b) round specimens used for constant stress amplitude axial fatigue testing.

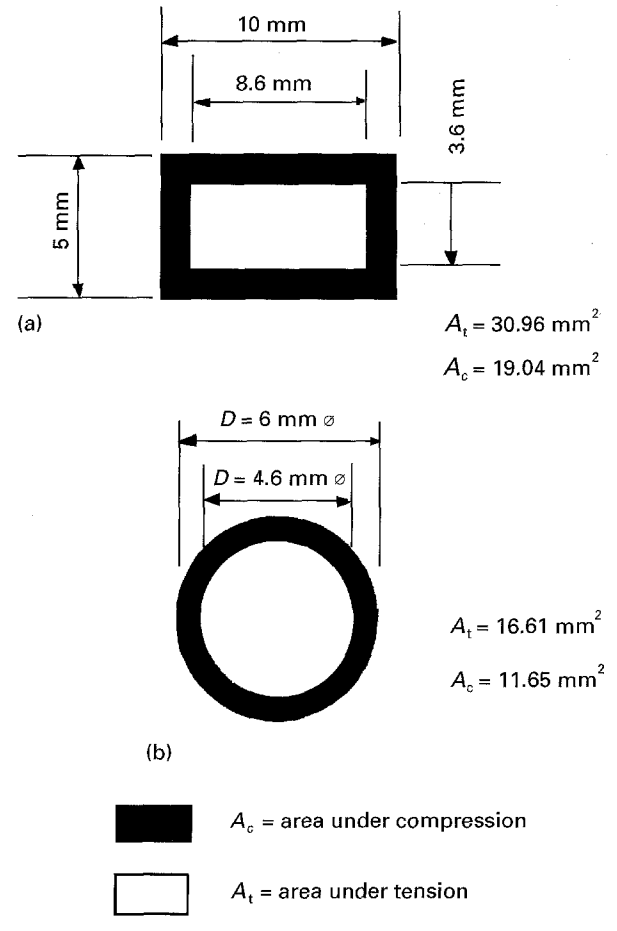

Figure 2 Areas under residual compressive and tensile stresses in flat and round specimens of IMI-685.

3.2. Fatigue tests

3.2.1. Room-temperature behaviour

Flat specimens of IMI-685 in the machined, polished and shot-peened (MPS) condition tested at a stress amplitude of 770 MPa ($\sigma_a/\sigma_{PS} = 0.755$; σ_a = applied stress amplitude, σ_{PS} = proof stress of the material) showed an increase in fatigue life of about 11% over specimens in the machined and polished (MP) condition (Table I). For round specimens, the increase was about 13% (Table II). Table II also reveals that at higher stress amplitudes, the fatigue life of the peened specimens decreased in comparison with that of the unpeened specimens. The percentage decrease, however, became less as the applied stress amplitude approached the proof stress of the material.

TABLE I Constant stress amplitude axial fatigue tests at room temperature on flat samples of IMI-685. $\sigma_a/\sigma_{ps} = 0.755$, σ_{PS} at room temperature = 1020 MPa

Material condition	Stress range (MPa)	Number of cycles at failure, N_f	Change (%)
MP	0–770	19 500	
	0–770	19 800	
MPS	0–770	21 600	+ 11
	0–770	22 000	

TABLE II Constant stress amplitude axial fatigue tests at room temperature on round specimens of IMI-685

Material condition	Stress range (MPa)	σ_a/σ_{PS}	Number of cycles at failure, N_f	Change (%)
MP	0–770	0.755	100 200	
MP	0–770	0.755	97 458	
MPS	0–770	0.755	112 000	+ 13
MPS	0–770	0.755	110 578	
MP	0–890	0.872	50 975	
MP	0–890	0.872	53 450	
MPS	0–890	0.872	27 948	− 46
MP	0–955	0.936	11 108	
MP	0–955	0.936	10 850	
MPS	0–955	0.936	8 467	− 25
MPS	0–955	0.936	8 100	

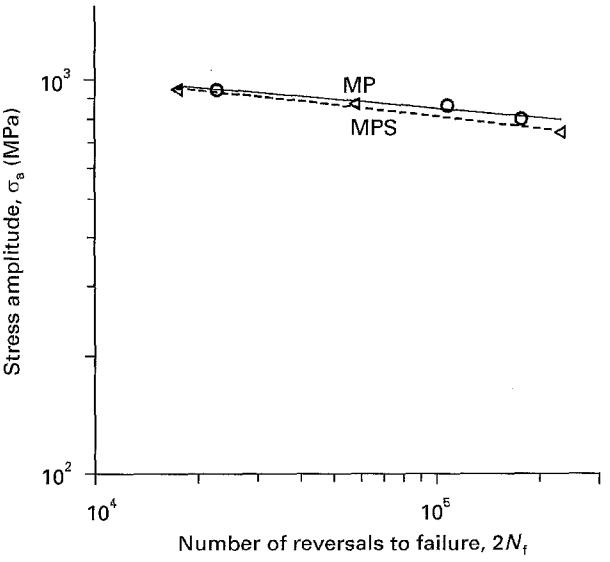

Figure 3 σ_a versus $2N_f$ relationship for the MP and MPS conditions, in specimen IMI-685 at room temperature.

A log–log plot of the stress amplitude, σ_a, against the number of reversals to failure, $2N_f$, was a straight line for IMI-685 in both the MP and MPS conditions (Fig. 3). This verified the modified Basquin equation

$$\sigma_a = \sigma_f'(2N_f)^b \quad (1)$$

where σ_f' is the fatigue strength coefficient and b is the fatigue strength exponent [2].

Table III shows the room-temperature fatigue data for IMI-318. Over the entire range of stress amplitudes employed, a reduction in the fatigue life to the tune of about 52%–55% was observed for the MPS condition in comparison with the MP condition. In this alloy also the modified Basquin equation was obeyed for both the MP and the MPS conditions (Fig. 4).

The values of the parameters σ_f', b and the calculated cyclic hardening exponent, n', for the two alloys derived from Figs 3 and 4, are presented in Table IV.

3.2.2. Elevated temperature fatigue behaviour

Only IMI-685 was used in the study. Behaviour at 200 °C was somewhat similar to what was seen at room temperature (Table V). However, at 450 °C for a σ_a/σ_{PS} ratio of 0.938, the fatigue life decreased by about 39% for the MPS condition compared with the MP condition. An increase in fatigue life of about 45% was registered for the MPS condition over the MP condition when the σ_a/σ_{PS} ratio was reduced to 0.870 (Table VI).

TABLE III Constant stress amplitude axial fatigue tests at room temperature on round specimens of IMI-318. σ_{PS} at room temperature = 930 MPa

Material condition	Stress range (MPa)	σ_a/σ_{PS}	Number of cycles at failure, N_f	Change (%)
MP	0–770	0.828	280 000	
MP	0–770	0.828	265 000	
MPS	0–770	0.828	120 600	
MPS	0–770	0.828	124 000	− 55
MP	0–833	0.896	58 731	
MPS	0–833	0.896	28 500	− 52
MP	0–890	0.957	29 810	
MP	0–890	0.957	31 500	
MPS	0–890	0.957	14 226	
MPS	0–890	0.957	13 740	− 54

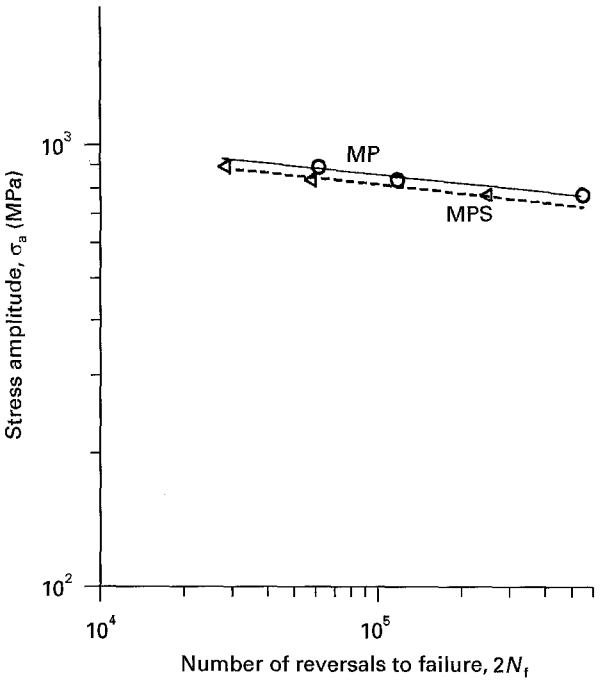

Figure 4 σ_a versus $2N_f$ relationship for the MP and the MPS conditions, in specimen IMI-318 at room temperature.

TABLE V Constant stress amplitude axial fatigue tests on round samples of IMI-685 at a test temperature of 200 ± 5 °C. σ_{PS} at 200 °C = 820 MPa

Material condition	Stress range (MPa)	σ/σ_{PS}	Number of cycles at failure, N_f	Change (%)
MP	0–710	0.866	24 367	
MPS	0–710	0.866	20 097	− 17
MPS			21 005	
MP	0–770	0.939	8 105	
MP			8 400	
MPS	0–770	0.939	7 500	− 6
MPS			7 800	

3.3. Fracture behaviour

Fig. 5 pertains to a flat IMI-685 sample in the MP condition (peak roughness, $R_Z = 0.99$ μm). Fracture appeared to start from a corner at the surface (arrowed in Fig. 5a) and propagated inwards. At higher magnification, the corner region was seen to consist of dimpled areas (arising from microvoid formation) and striations (shown bounded by arrows in Fig. 5b). Fig. 5c displays a corner crack at some distance from

TABLE IV Values of the room-temperature fatigue strength coefficient, fatigue strength exponent and calculated cyclic strain-hardening exponent for IMI-685 and IMI-318

Material	Material condition	Fatigue strength coefficient, σ_f' (MPa)	Calculated cyclic hardening exponent, $n'[b = -n'/(1 + 5n')]$	Fatigue strength exponent, b
IMI-685	MP	1600	0.108	− 0.070
	MPS	2000	0.139	− 0.082
IMI-318	MP	2000	0.101	− 0.067
	MPS	2000	0.117	− 0.074

TABLE VI Constant stress amplitude axial fatigue tests on round samples of IMI-685 at a test temperature of 450 ± 5 °C. σ_{PS} at 450 °C = 650 MPa

Material condition	Stress range (MPa)	σ_a/σ_{PS}	Number of cycles at failure, N_f	Change (%)
MP	0–565	0.870	170436	
MP		0.870	180450	
MPS	0–565	0.870	260400	+ 45
MPS		0.870	245600	
MP	0–610	0.938	15780	
MP		0.938	16250	
MPS	0–610	0.938	9306	− 39
MPS		0.938	10104	

the fracture surface. Dimpled as well as featureless regions are seen in Fig. 5d which pertains to a round sample of IMI-685 in the MP condition. Thus, in this alloy, even in the MP condition, ductile as well as brittle fracture features could be seen.

Flat samples of IMI-685 in the MPS condition (R_Z = 7.88 μm) displayed dimples of larger size (Fig. 6a) compared with the MP condition. Fatigue failure originated at the surface and/or at the notches/dents caused by shot peening (Fig. 6b, c). The constraining effects of the notches/dents on plastic deformation is also seen in Fig. 6c, which shows flat areas with steps in the vicinity of a crack – often interpreted as evidence for the inward propagation of cracks by cleavage.

In IMI-318 alloy in the MP condition (R_Z = 0.76 μm) also, fatigue cracks originated at the surface (Fig. 7a), but the fracture appeared more ductile than in IMI-685 alloy in the MP condition (cf.

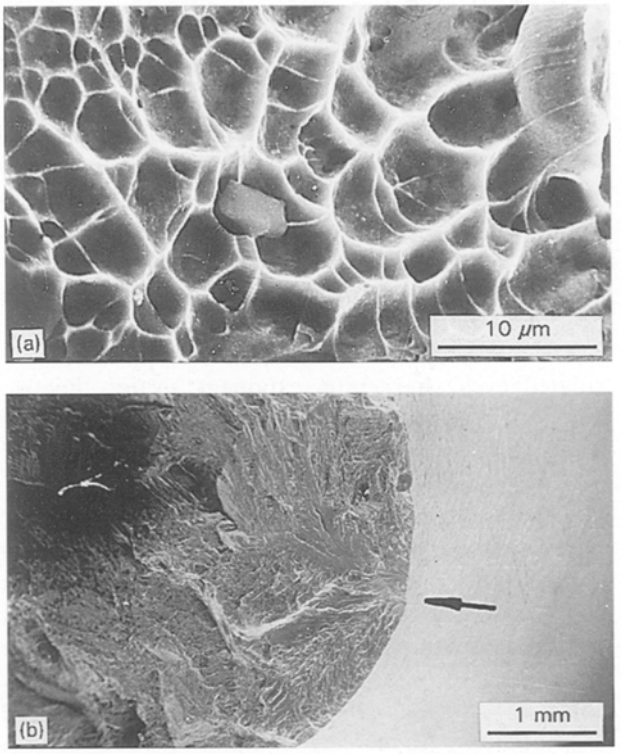

Figure 6 SEM fractographs of a flat sample of IMI-685 in the MPS condition (room temperature, stress range 0–770 MPa, 21 600 cycles to failure). (a) Large dimples, (b) surface origin of fatigue crack, (c) crack and step formation at a dent caused by peening.

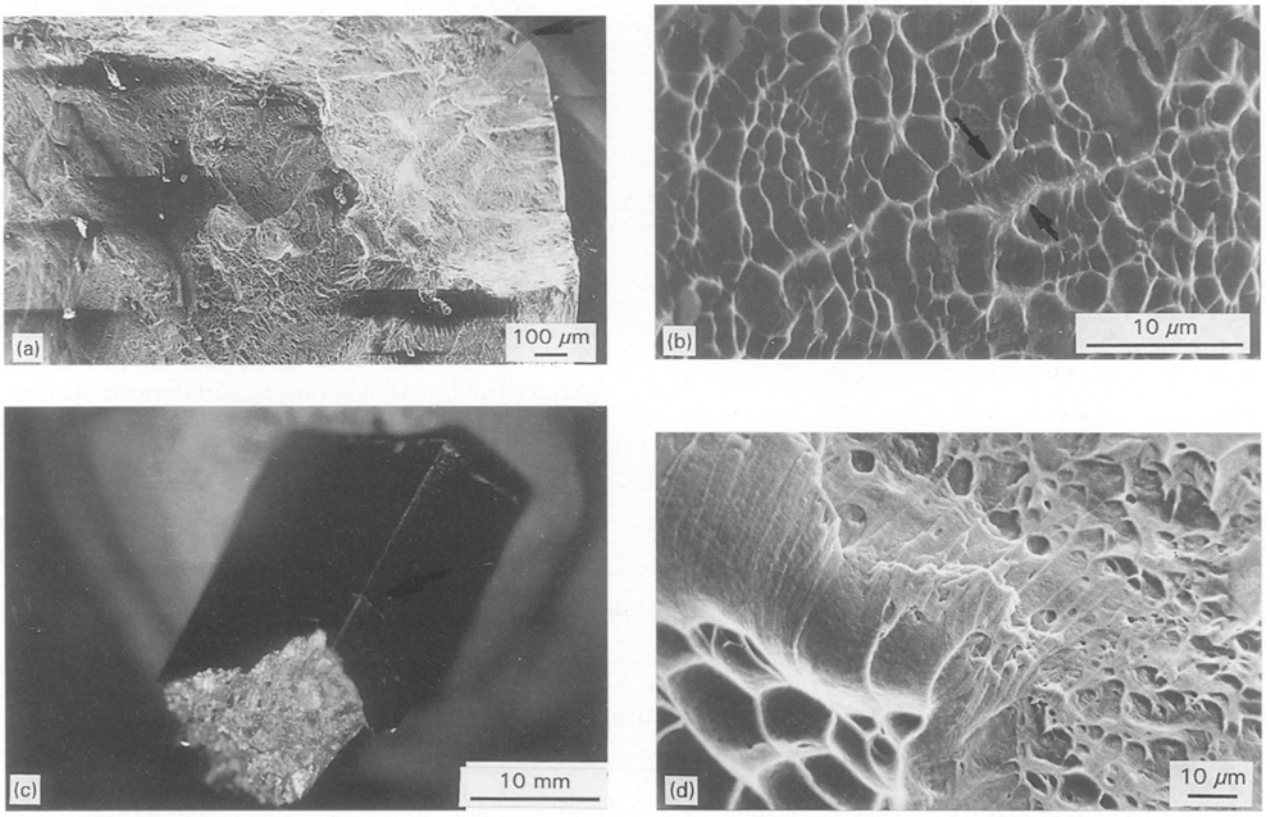

Figure 5 SEM fractographs of a flat sample of IMI-685 in the MP condition (room temperature, stress range of 0–770 MPa, 19 600 cycles to failure). (a) Crack origin at a corner, (b) dimpled areas and striations, (c) a macrograph showing a corner crack, (d) a round specimen in the MP condition revealing dimpled and featureless regions.

Figure 6 (continued.)

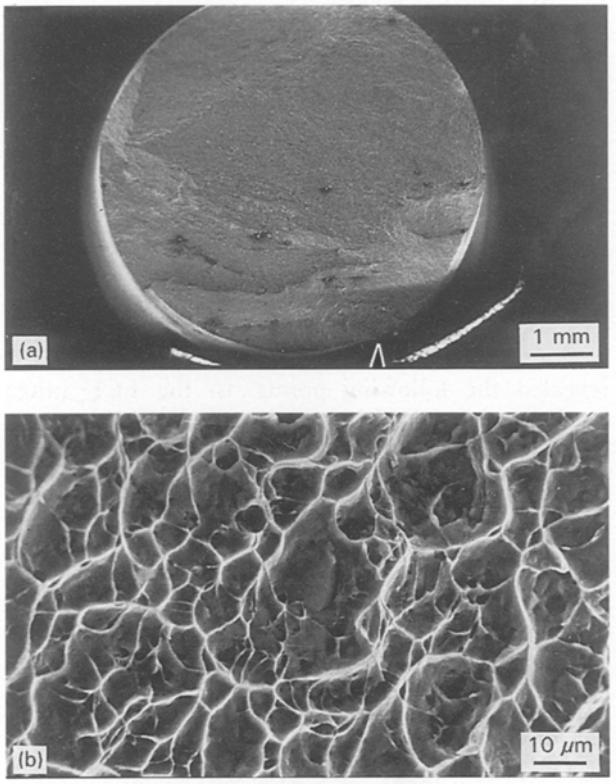

Figure 7 SEM fractographs of a round sample of IMI-318 in the MP condition (room temperature). (a) Surface origin of a fatigue crack (arrowed), and (b) fully dimpled region of fracture.

Figs 7b and 5d). In the MPS condition (R_Z = 5.66 μm) the notches/dents produced by the peening gave rise to a cleavage type of fracture in the vicinity of the crack origin (Fig. 8a). The fracture surface was largely made up of cleavage facets (Fig. 8b).

4. Discussion

4.1. Fatigue behaviour

A comparison of Tables II, V and VI pertaining to the round specimens of IMI-685 revealed the following points.

(i) At a fixed σ_a/σ_{ps} ratio, the fatigue lives at 200 °C had decreased for both the MP and the MPS conditions when compared with the results corresponding to room temperature – a normal temperature effect on fatigue life.

(ii) At 450 °C, the fatigue lives at a fixed (σ_a/σ_{PS}) ratio for both the MP and the MPS conditions were greater than at either room temperature or at 200 °C. This anomalous behaviour is traceable to dynamic strain ageing (DSA) present in this material at this temperature [3]. It is known that DSA enhances the fatigue life [4, 5]. The present results reveal that the effect of DSA in increasing the fatigue life becomes more pronounced at lower σ_a/σ_{PS} ratios.

Both IMI-685 and IMI-318 were found to obey the modified Basquin equation in the MP as well as the MPS conditions (Figs 3 and 4). The values of σ_f', b and n' for IMI-685 in the MP condition presently obtained (Table IV) agreed well with those of an earlier study [6]. σ_f' nearly equals the fracture stress of a material [2]. A higher value for the same (2000 MPa) in IMI-685 in the MPS condition compared with the MP condition (1600 MPa) indicates that shot peening increased the extent of work hardening before fracture. On the other hand, the identical values of σ_f' (2000 MPa) found for IMI-318 in both the MP and the MPS conditions is traced to the extensive relaxation of the residual stresses in IMI-318 on cyclic loading [3] which had practically nullified the effect of shot peening.

In IMI-685, at room-temperature, glass-bead peening introduced at the surface a maximum compressive residual stress, σ_{LP}, of -700 MPa [1]. Compressive residual stresses enhance the resistance to both crack initiation and propagation. However, results presented in Tables I and II reveal that the fatigue life in the MPS condition was superior to that in the MP condition only when the ratio σ_{LP}/σ_a was greater than or equal to about 0.92. This finding is in conformity with earlier results [7, 8]. The low-level increase in the fatigue life (11%–13%) for the MPS condition, on the other hand, could be due to the size effect [7] as the

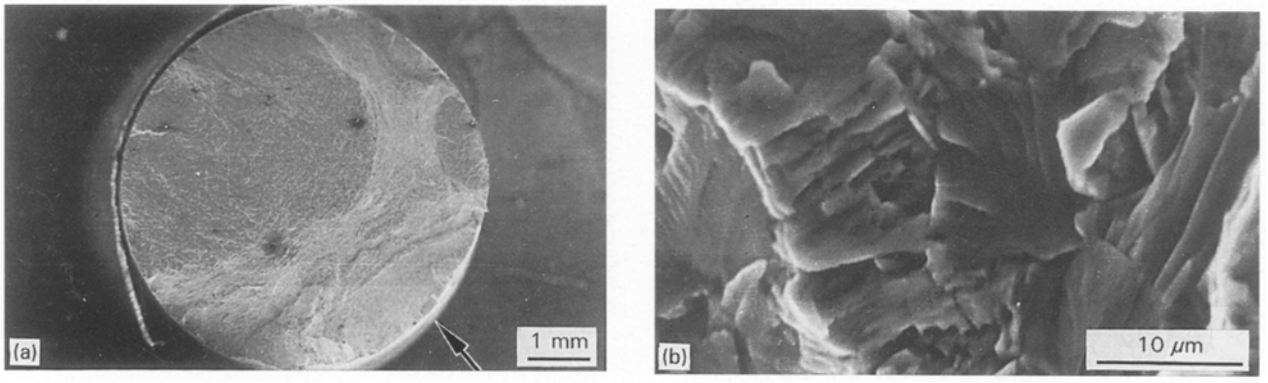

Figure 8 SEM fractographs of a round sample of IMI-318 in the MPS condition (room temperature). (a) Surface origin of a fatigue crack (arrowed), (b) a cleavage type of fracture near the crack origin.

specimens were taken from industrial-scale high-pressure compressor discs of gas turbines.

Residual stresses present in materials can significantly relax under high cyclic stresses [3, 9–14]. In IMI-685 in the stress range of 0–770 MPa, stress relaxation at the surface (where fatigue fracture originated) was marginal [3]. Therefore, in this range the fatigue life increased following shot peening. However, at high stress ranges stress relaxation was considerable. In these ranges, the increased surface roughness resulting from shot peening promoted early initiation of fatigue cracks [15–17] and there was a decrease in the fatigue life following shot peening.

Materials like IMI-685 display good crack propagation resistance but poor crack initiation resistance [18–21].

In the low-cycle fatigue (LCF) range, when the cyclic stress amplitude is close to the proof stress of the material, the total life is almost entirely governed by crack propagation. At lower cyclic stress amplitudes, the fatigue life partitions between crack initiation and propagation. Moreover, the notch effects due to glass-bead peening adversely affect crack initiation without having much effect on crack propagation. However, in this range at higher stress amplitudes, the blunting of the root of the notch left by peening is likely to be greater than at lower stress amplitudes [22]. Taken together, these features could lead in the LCF range to a higher percentage reduction in the fatigue life as a result of glass-bead peening at lower cyclic stress amplitudes than at higher cyclic stress amplitudes. This line of argument is verified by the present results.

In the high-cycle fatigue (HCF) range, the notch effect due to glass-bead peening was not severe, as the surface compressive residual stresses resulting from peening were practically unrelaxed. Thus, crack initiation was not advanced and the compressive residual stresses delayed crack propagation and this resulted in an increase in the fatigue life. An improvement in life by 11%–13% at a peening intensity of 35 N observed here is in accordance with the argument presented earlier for medium intensity (33 N) peening [23].

For titanium alloys, a rule of thumb has been evolved that A_t/A_c should be greater than or equal to 20 [24]. Then, up to 5% of the specimen cross-section can be under compression to provide increased crack initiation and/or propagation resistance, while the remaining 95% of the cross-section can distribute the tensile load and minimize the formation of internal defects and stress raisers.

From Fig. 2 it is clear that in the present experiments the A_t/A_c ratio was only 1.6 and 1.4, respectively, for the flat and round specimens. Thus, the elimination of stress raisers during fatigue deformation could not have been effective, and as the subsurface tensile residual stresses relaxed more readily than surface compressive residual stresses [1, 3], the fatigue crack originated at the specimen surface in all cases.

From Tables I and II, the effect of specimen geometry on the fatigue life of IMI-685 can be inferred and this is in accordance with earlier results [25]. As the flat specimens approximately represent the shape of the compressor blades of gas turbine engines, they indicate at least roughly the likely changes in the fatigue life of the blades following glass-bead peening.

Thermal relaxation of residual stresses in titanium starts only at around 280 °C [26]. Therefore, the lower percentage reduction in fatigue life at 200 °C following glass-bead peening compared with that seen at room temperature (a 6% reduction against a 25% reduction at $\sigma_a = 770$ MPa, $\sigma_a/\sigma_{PS} = 0.94$) is traced to the reduced effect of the notches produced by peening at the higher temperature. Significant thermal relaxation of the residual stresses, on the other hand, led to a decrease in the fatigue life by 39% at 450 °C for a σ_a/σ_{PS} ratio of 0.94. At a σ_a/σ_{PS} ratio of 0.87, however, the beneficial effects of an increased dislocation density caused by peening [27, 28] and dynamic strain ageing, overcame the detrimental effect of the thermal relaxation of the residual stresses and led to an enhanced fatigue life (Table VI).

The drastic reduction (by 52%–55%) in the 10^5 cycle fatigue life of IMI-318 (stress range 0– 770 MPa) is a natural consequence of the extensive relaxation of the residual stresses [3, 29, 30] and the detrimental effects of the surface damage caused by peening.

A comparison of the room-temperature fatigue behaviour of IMI-685 (Table II) with that of IMI-318 revealed the following points. In the LCF range ($< 10^5$ cycles), when the $(\sigma_{LP}/\sigma_a) \leqslant 0.92$, IMI-318 had a shorter fatigue life than IMI-685. But when (σ_{LP}/σ_a) ratio was greater than 0.92, the fatigue lives at different stress amplitudes of IMI-318 were far greater than those of IMI-685 for both the peened and unpeened conditions.

Acicular microstructures, e.g. as seen in IMI-685 [3] confer superior crack propagation resistance compared to equiaxed microstructures as present in IMI-318 [18–21]. Thus, it would appear that crack propagation rather than crack initiation controls the LCF life of IMI-318. The lower yield stress of IMI-318 in comparison with that of IMI-685 (930 MPa versus 1020 MPa) could have also been partly responsible for the inferior LCF life of IMI-318. (A lower yield stress reduces the crack initiation resistance in the LCF range, where the applied stress is of the order of the proof stress.)

In the HCF range, however, an equiaxed microstructure confers superior crack initiation resistance and so the fatigue life of IMI-318 is greater than that of IMI-685.

The lower n' (Table IV) and the greater ductility of IMI-318 at room temperature compared with IMI-685 [25, 31] might have caused higher cyclic strains at a specified stress amplitude in the former alloy than in the latter. Then, for a fixed stress ratio, a higher percentage reduction in the fatigue life of a peened specimen compared with that of an unpeened sample, may be expected in the case of IMI-318 than in IMI-685 and this is what has been observed.

4.2. Fracture behaviour

The flat areas with steps in the region of a crack seen in IMI-685 in the MPS condition (Fig. 6c) is perhaps

due to the tendency of cracks to propagate through a given α packet in a straight line parallel to the (plastic deformation) slip bands [32]. Crack propagation is by transgranular cleavage through the α and β phases. The steps then can be associated with the boundaries between the adjacent phases. The lower peak roughness of IMI-318 in the MPS condition ($R_Z = 5.66$ μm) compared with IMI-685 in the MPS condition ($R_Z = 7.88$ μm) could have been one of the factors that gave rise to a higher HCF life in the former alloy than in the latter.

5. Conclusions

Based on an experimental investigation of the fatigue and fracture behaviour of the two titanium alloys IMI-685 and IMI-318 the following conclusions could be drawn.

1. In both the alloys in the MP as well as the MPS conditions, the modified Basquin equation was obeyed.

2. The alloys in the MPS condition showed reductions in fatigue life at high stress amplitudes. This was because at these stress amplitudes extensive relaxation of the shot-peen-induced residual stresses was present and the surface damage caused by peening lowered the crack initiation resistance. Moreover, in this range, the crack propagation resistance remained unchanged from that of the MP condition.

3. The percentage reduction in the fatigue life of IMI-685 in the MPS condition decreased when the cyclic stress amplitude approached the proof stress of the material. This was attributed to the reduced effect of shot-peen-induced notches with increasing stress amplitude.

4. In IMI-685 in the MPS condition, the fatigue life increased when the (σ_{LP}/σ_a) ratio was greater than or equal to 0.92.

5. The decrease in the fatigue life of IMI-318 in the MPS condition at all stress amplitudes was traced to the significant relaxation of the peen-induced residual stresses during the fatigue deformation.

6. The reduction in the fatigue life of IMI-685 in the MPS condition at 450 °C and high stress amplitudes is attributed to the significant thermal relaxation of the residual stresses and the surface damage caused by peening.

7. The improvement in the fatigue life of IMI-685 in the MPS condition at 450 °C and relatively low cyclic stress amplitudes, on the other hand, is traced to the less significant relaxation of the residual stresses and the beneficial effects of a higher dislocation density in the shot-peened layers and dynamic strain ageing.

8. In both the alloys in the MPS as well as MP conditions, fracture originated at the specimen surface.

9. In IMI-685 in the MPS condition, the dimple size on the fracture surface was larger whenever the fatigue life was greater for this condition, than for the MP condition.

10. Fracture in the surface layers of both the alloys had a more brittle appearance for the MPS condition than for the MP condition.

Acknowledgements

The authors thank Dr. R. Krishnan, Director, Gas Turbine Research Establishment, Bangalore, for encouragement. K. A. Padmanabhan thanks the Alexander von Humboldt – Stiftung, Bonn, for a "Forschungspreis" at the T. H. Darmstadt, Department of Materials Science, during which period this paper was finalized.

References

1. B. R. SRIDHAR, W. G. NAFDE and K. A. PADMANABHAN *J. Mater. Sci.* **27** (1992) 5783.
2. G. E. DEITER, "Mechanical Metallurgy" (McGraw-Hill, Singapore, 1986) p. 392.
3. B. R. SRIDHAR, PhD thesis, Indian Institute of Technology, Madras (1994).
4. A. T. K. ASSADI, H. M. FLOWER and D. R. F. WEST, *Metals Technol.* **6** (1979) 8.
5. Y. KRISHNA MOHANA RAO and C. RAMACHANDRA, personal communication (1992).
6. P. RAMA RAO, personal communication (1992).
7. M. N. STEPNOV, M. G. VEITSMAN, E. V. GIATSINOU, L. V. AGAMISOU and L. N. GUSKOVA, *Probl. Prochn.* **3** (1985) 20–23; cited in *Met. Abs.* (31–4339) Vol. 18, October 1985.
8. P. O'HARA, in "Impact Surface Treatment", Second International Conference on Impact Treatment Processes, edited by S. A. Meguid (Elsevier Applied Science, London, New York, 1986) pp. 115–26.
9. T. HIRSCH, O. VOHRINGER and E. MACHERAUCH, in "Proceedings of the Second International Conference on Shot Peening" (ICSP-2, Chicago, IL), edited by H.O. Fuchs (American Shot Peening Society, NJ, 1984), pp. 90–101.
10. N. SKALLI and J. F. FLAVNOT, *Journees Int. Pring. S. F. M.* (1984) pp. 98–117, cited in "Impact Surface Treatment", Second International Conference on Impact Treatment Processes, edited by S. A. Meguid (Elsevier Applied Science, London, New York, 1986) pp. 45–56.
11. S. KONDAMA, in "Proceedings of the International Conference on Mechanical Behaviour of Materials", Kyoto, Vol. 2 (1971) pp. 111–118, cited in "Impact Surface Treatment", Second International Conference on Impact Treatment Processes, edited by S. A. Meguid (Elsevier Applied Science, London, New York, 1986) pp. 45–56.
12. M. DESVIGNES, B. GENTIL and L. CASTEX, in "Impact Surface Treatment", Second International Conference on Impact Treatment Processes, edited by S. A. Meguid (Elsevier Applied Science, London, New York, 1986) pp. 45–56.
13. J. BERGSTROM and T. ERICSSON, in "Proceedings of the Second International Conference on Shot Peening" (ICSP-2, Chicago, IL), edited by H. O. Fuchs (American Shot Peening Society, NJ, 1984), pp. 241–48.
14. J. BERGSTROM, "Advances in Surface Treatment Technology Applications", Vol. 3, "Effects" (Pergamon Press, London, 1986) pp. 97–112.
15. Q. QIU, X. LI, and R. WANG, in "Microstructure and Mechanical Properties of Materials", Vol. II (Conference Proceedings, China, October 1985) pp. 733–40, cited in *Met. Abs.* (31-4854) Vol. 20, November 1987, p. 48.
16. M. TIKTINSKY, in "The Science, Technology and Applications of Titanium", edited by R. I. Jaffee and N. V. Promisel (Pergamon Press, London, 1970) p. 1013.
17. G. S. WAS and R. M. PELLOUX, *Metall. Trans.* **10A** (1978) 1339.
18. H. MARGOLIN, M. A. GREENFIELD and I. GREENHUT, in "Titanium science and Technology", Vol. 3 (Conference Proceedings), edited by R. I. Jaffee and H. M. Burte (Plenum Press, New York, London, 1973) p. 1709.
19. D. EYLON, J. A. HALL, C. M. PIERCE and D. L. RUCKLE, *Metall. Trans.* **7A** (1976) 1817.
20. R. MARRISEN, M. PETERS, K. SCHULTE, K. H. TRAUTMAN and H. NOWACK, in "Titanium Science and

Technology", Vol. 4, Fifth International Conference on Titanium, edited by G. Luetjering, W. Zwicker and W. Bunk (Deutsche Gesellschaft fur Metallkunde, Oberursel, 1984) pp. 2289–96.
21. R. MARRISEN, M. PETERS, K. SCHULTE, K. H. TRAUTMAN and K. MULL, Deutsche Forchungs Versuchsanstalt Luft Raumfahrt (FRG) N87-11885/7/GAR, May 1986, p. 42, cited in *Met. Abs.* (31-3978) Vol. 20, September 1987, p. 62.
22. L. F. IMPELLIZZERI, "Cumulative Damage Analysis in Structural Fatigue", Effects of Environment and Complex Load History on Fatigue Life, ASTM Special Technical Publication 462 (American So ciety for Testing and Materials, Philadelphia, PA, 1970) pp. 40–68.
23. B. GILLESPE, "Titanium-1986, Products and Applications", Vol. I, Proceedings of the Technical Programme from 1986 International Conference (Titanium Development Association, Dayton, USA, 1987), pp. 154–64.
24. V. J. ERDEMAN and R. D. RADCLIFFE, Effects of Shot Peening on the Cyclic Behaviour of Thermally Exposed and Non-thermally Exposed Titanium Alloys, in "Canadian Materials and Processing Technology Conference and Exposition", September 1969.
25. Titanium Alloy IMI-685, Technical Data bulletin from Imperial Metal Industries (Birmingham, UK, 1983).
26. O. VOHRINGER, T. HIRSCH and E. MACHERAUCH, in "Titanium Science and Technology", Vol. 4, Fifth International Conference on Titanium, edited by G. Luetjering, W. Zwicker and W. Bunk (Deutsche Gesellschaft fur Metallkunde, Oberursel, 1984) pp. 2203–10.
27. C. GERDES and G. LUETJERING, in "Proceedings of the Second International Conference on Shot Peening" (ICSP-2, Chicago, IL), edited by H. O. Fuchs (American Shot Peening Society, NJ, 1984) pp. 175–80.
28. L. WAGNER and G. LUETJERING, in "First International Conference on Shot Peening", edited by Nicku-Lari (Pergamon Press, New York, 1981) p. 453.
29. *Idem*, in "Second International Conference on Shot Peening (ICSP-2, Chicago, IL), Proceedings of the Second International Conference on Shot Peening" (ICSP-2), edited by H. O. Fuchs (American Shot Peening Society, NJ, 1984) pp. 194–200.
30. *Idem, ibid*, pp. 201–7.
31. Titanium Alloy IMI-318, Technical Data Bulletin from Imperial Industries, (Birmingham, UK, 1971).
32. P. LEHR, in "Titanium Science and Technology", Vol. 3, Proceedings of the Fourth International Conference on Titanium, edited by H. Kimura and O. Izumi (Metallurgical Society of AIME, Warrendale, PA, 1980) p. 1617.

Received 8 January
and accepted 24 April 1996